Aqueous Solvation of a Rubredoxin Redox Site Analog: A Molecular Dynamics Simulation

Yang Yang,† Brian W. Beck, Vaishali S. Shenoy, and Toshiko Ichiye*

Contribution from the Department of Biochemistry/Biophysics, Washington State University, Pullman, Washington 99164-4660

Received October 5, 1992

Abstract: A molecular dynamics simulation of $Fe(SCH_2CH_3)_4^-$, a redox site analog of the iron–sulfur protein rubredoxin, in aqueous solution has been performed. In this simulation, an average of 2.3 water molecules are able to penetrate the tetrahedral structure of the Fe–S site at an average distance of about 3.6 Å from the Fe, each with a hydrogen pointing toward the Fe. Moreover, the degree of penetration is determined by the C–S–Fe–S dihedral angles, since the CH_2 group can block the approach to the Fe. In addition, there are about 4.4 water molecules near each sulfur with a preference for bifurcated hydrogen bonds to the sulfur. Rubredoxin provides a similar though less polar immediate environment for the Fe in that, although it excludes water from the Fe, it has two amide nitrogens at about the same distance from the Fe as the innermost waters, and each sulfur has three nearby amides, with two of the sulfurs having one N–H···S bond each and two of the sulfurs having two N–H···S bonds each. The protein also constrains the C–S–Fe–S dihedral angles, thus determining how close a polar group can approach, and these angles are different from those of $[Fe(S_2\text{-}o\text{-}xyl)_2]^-$, the best synthetic analog for the redox site. In addition, analogs with the same C–S–Fe–S dihedral angles as the protein appear to have a substantially different electrostatic potential at the Fe than those with the same angles as $[Fe(S_2\text{-}o\text{-}xyl)_2]^-$.

Introduction

Studies of analogs of redox proteins are of great importance in understanding the role of the protein environment in determining the redox properties of the redox site. The work here is on an analog of rubredoxin (Rd), an iron–sulfur redox protein.[1] Rubredoxins are small proteins (molecular weight 5000–20 000) with a redox site consisting of a single Fe surrounded tetrahedrally by four sulfur atoms, which are from conserved cysteine residues. There is a wealth of experimental data, including a high-resolution crystal structure (1.2 Å) for *Clostridium pasteurianum* Rd (molecular weight ~6100).[2]

Experimentally, an analog of the Rd redox site, $[Fe(S_2\text{-}o\text{-}xyl)_2]^-$, has been synthesized by Holm, Ibers, and co-workers.[3] Crystal structures of the oxidized and reduced forms show that there are small changes in bond lengths and bond angles upon reduction and that the structure is similar to the redox site of Rd.[3] The redox potential of $[Fe(S_2\text{-}o\text{-}xyl)_2]^-$ in DMF has been measured to be –0.8 eV (as compared to –0.056 eV for Rd).[3] This analog by itself is not soluble in aqueous solution, but it and Fe(II) complexes with cysteine-containing peptides have been solubilized in aqueous Triton X-100 micelle solutions.[4] Resonance Raman and infrared studies of $[Fe(S_2\text{-}o\text{-}xyl)_2]^{-,2-}$ and Rd indicate that the spectroscopy can be explained only by models which include the entire cysteine side chain; *i.e.*, for $Fe(SR)_4^{-,2-}$, R must be at least CH_2CH_3, because the Fe–S–CH_2–CH_3 dihedral angle determines some of the spectral features.[5]

The redox site of Rd has been the subject of several electronic structure calculations because of its relatively small size. One study involved *ab initio* quality Hartree–Fock and extensive configuration interaction studies of the ground and excited states of $Fe(SH)_4^{-,2-}$.[6] Another study involved Xα valence bond scattered wave calculations for $Fe(SR)_4^{-,2-}$ where R = H, CH_3.[7] Among other things, these results indicate that the Mossbauer shifts, which can be linearly related to the electronic charge density at the Fe, are substantially smaller for R = CH_3 than for R = H.

The experimental and theoretical studies of the Rd analogs have not addressed the question of the microscopic interaction between the analog and the solvent environment, even though this is critical when attempting to compare the electrostatic environment in solution and in the protein. Molecular dynamics simulations provide a theoretical method to study this interaction. In particular, since no analogs of the FeS_4 site have been synthesized which are soluble in water without detergent, simulations can be used to study how the environment of the redox site differs between the protein in water and a soluble analog in water and thus address questions as to the role of the protein matrix.

Here we present results of a classical molecular dynamics simulation of the oxidized form of an analog of the Rd redox site, $Fe(SCH_2CH_3)_4^-$, in aqueous solution. The focus is on the structure of the surrounding water, which will influence the redox potential. In addition, the structure of the analog itself is described.

Methods

$Fe(SCH_2CH_3)_4^-$ was simulated with 985 waters in a cubic box of length 31.034 Å using periodic boundary conditions. The calculations were performed using the macromolecular mechanics/dynamics program, CHARMm (version 21.2).[8] The simulation was for the system in the microcanonical ensemble at a temperature of approximately 300 K. The

* Author to whom correspondence should be addressed.
† Present address: Biosym Technologies Inc., 9685 Scranton Rd., San Diego, CA 92121-2777.

(1) Lovenberg, W., Ed. *Iron-Sulfur Proteins*; Academic Press: New York, 1973, 1973, and 1977; Vols. 1–3. Spiro, T. G., Ed. *Iron-Sulfur Proteins*; Wiley-Interscience: New York, 1982.
(2) Watenpaugh, K. D.; Sieker, L. C.; Jensen, L. H. *J. Mol. Biol.* **1979**, *131*, 509; *Ibid.* **1980**, *138*, 615.
(3) Reviewed by Holm and Ibers: Holm, R. H.; Ibers, J. A. In *Iron-Sulfur Proteins*; Lovenberg, W., Ed.; Academic Press: New York, 1977; p 205. Lane, R. W.; Ibers, J. A.; Frankel, R. B.; Papaefthymiou, G. C.; Holm, R. H. *J. Am. Chem. Soc.* **1977**, *99*, 84.
(4) Nakata, M.; Ueyama, N.; Fuji, M.-A.; Nakamura, A.; Wada, K.; Matsubara, H. *Biochim. Biophys. Acta* **1984**, *788*, 788.
(5) Yachandra, V. K.; Hare, J.; Moura, I.; Spiro, T. G. *J. Am. Chem. Soc.* **1983**, *105*, 6455. Czernuszewicz, R. S.; LeGall, J.; Moura, I.; Spiro, T. G. *Inorg. Chem.* **1986**, *25*, 696.
(6) Bair, R. A.; Goddard, W. A. *J. Am. Chem. Soc.* **1978**, *100*, 5669.
(7) (a) Noodleman, L.; Norman, J. G.; Osborne, J. H.; Aizman, A.; Case, D. A. *J. Am. Chem. Soc.* **1985**, *107*, 3418. (b) Norman, J. G., Jr.; Jackels, S. C. *J. Am. Chem. Soc.* **1975**, *97*, 3833.
(8) Polygen version: Brooks, B. R.; Bruccoleri, R. E.; Olafson, B. D.; States, D. J.; Swaminathan, S.; Karplus, M. *J. Comput. Chem.* **1983**, *4*, 187.

0002-7863/93/1515-7439$04.00/0

Verlet algorithm was used to propagate the dynamics, and a time step of 0.001 ps was used.

The potential energy function combined parameters from CHARMM19 plus additional parameters for the Fe–S site. The parameters were chosen to be consistent with those used for other calculations of Rd which are being carried out. The CH_2 and CH_3 groups are treated via the extended atom model in which hydrogens are included as part of the heavy atom to which they are attached. For the Fe–S site, equilibrium bond lengths and bond angles were taken from a crystal structure of $Et_4N[Fe(S_2\text{-}o\text{-}xyl)_2]$[3] and force constants were modified to fit the CHARMM potential energy function from those of Spiro *et al.*, which were based on their spectroscopic data.[5] Normal mode calculations were carried out to verify the fit to the same spectroscopic data. Partial charges of the Fe–S site were taken from electronic structure calculations;[7] there is a charge of –0.05 on the Fe, –0.2 on the four sulfurs, and –0.0375 on the four CH_2 groups. The parameters for the Fe–S site are summarized in ref 9. The energy parameters for the water are from the TIP3P model.[10]

All electrostatic interactions were reduced smoothly to 0 by applying a switching function for separations of molecular centers between 6.5 and 7.5 Å. All van der Waals interactions were shifted to 0 at 7.5 Å. Nonbonded interactions were calculated only for atoms separated by less than 8 Å, using a list which was updated every 20 steps. Because of the short cutoffs, only features of the innermost shell were studied. Although Ewald sums have been shown to be more accurate than switching functions for charged systems in aqueous solutions,[11] these simulations will eventually be compared with simulations of net-charged proteins and the system must be net neutral for Ewald sums to be used. Since it is not clear that a net neutralizing background[11a] is appropriate for proteins nor is it feasible to equilibrate counterions in such a large system, switching functions were used here.

The initial structure of $Fe(SCH_2CH_3)_4^-$ was based on that of the Fe–S site in the crystal structure of rubredoxin,[2] which was relaxed via 100 steps of steepest descents minimization, and the structure of the water was taken from a previously equilibrated box of pure water at 1 g cm^{-3}. Coordinates of the analog and the water were superimposed, and, after removing overlapping waters, initial velocities for the entire system were assigned from a Maxwell–Boltzmann distribution at 300 K. The velocities were reassigned every 0.2 ps for 2 ps and then were rescaled to 300 K every 0.2 ps for another 2 ps. The system was allowed to evolve for another 70 ps without intervention. Equilibration was achieved within 14 ps of the initial velocity assignments so that the final 60 ps were used for the production part of the simulation.

Results

(a) Structure of the Analog. The average bond lengths and bond angles of the analog fluctuate very little during the course of the simulation. For instance, the Fe–S bonds have an average value of 2.26 ± 0.06 Å and the tetrahedral arrangement of the Fe–S site is preserved with average angles of S^1–Fe–S^2 = 110 ± 5°, S^1–Fe–S^3 = 109 ± 5°, S^1–Fe–S^4 = 109 ± 5°, S^2–Fe–S^3 = 109 ± 5°, S^2–Fe–S^4 = 111 ± 5°, and S^3–Fe–S^4 = 109 ± 5°. The dihedral angles C^n–C^n–S^n–Fe each undergo one to two dihedral transitions during the course of the simulation.

The solvent accessibility of the Fe is determined in large part by the values of the dihedral angles C^m–S^m–Fe–S^n. As we will see below, water molecules may penetrate the tetrahedral structure in the gap at the center of the triangle defined by any three of the sulfurs. Each face is defined by the three sulfurs which form the face, so that S^2:S^3:S^4 is made up of S^2, S^3, and S^4. A CH_2 group will tend to block this approach for the triangle formed by the sulfur to which the CH_2 is attached and the two sulfurs to which it is *gauche*. In other words, if C^1 is *trans* to S^4, the face S^1:S^2:S^3 is blocked by C^1. A given face may be blocked by zero to three CH_2 groups. There are a variety of structures which are consistent with these angles, two of which are illustrated in Figure 1. In this figure, a ball-and-stick representation is given to clarify the dihedral angles and a space-filling representation is given to demonstrate how a face is blocked. In the protein, each of the four faces is partially blocked by one CH_2, since the angles C^4–S^4–Fe–S^1, C^1–S^1–Fe–S^4, C^3–S^3–Fe–S^2, and C^2–S^2–Fe–S^3 (in the protein, the superscript 1 refers to Cys 6, 2 to Cys 9, 3 to Cys 39, and 4 to Cys 42) are all *trans* (Figure 1a). In the experimentally synthesized Holm–Ibers analog $[Fe(S_2\text{-}o\text{-}xyl)_2]^{-,2-}$, C^1–S^1–Fe–S^4 and C^4–S^4–Fe–S^1 are rotated to –60° so now two of the four faces are free while the other two are blocked by two CH_2 groups, since C^1–S^1–Fe–S^3, C^2–S^2–Fe–S^3, C^3–S^3–Fe–S^2, and C^4–S^4–Fe–S^2 are all *trans* (Figure 1b).

In the simulation, the starting structure begins with the same dihedral angles as in the protein. However, in the first 2 ps of the equilibration period, C^1–S^1–Fe–S^4 makes a transition to about –60°, as in the synthetic analog $[Fe(S_2\text{-}o\text{-}xyl)_2]^-$. During the

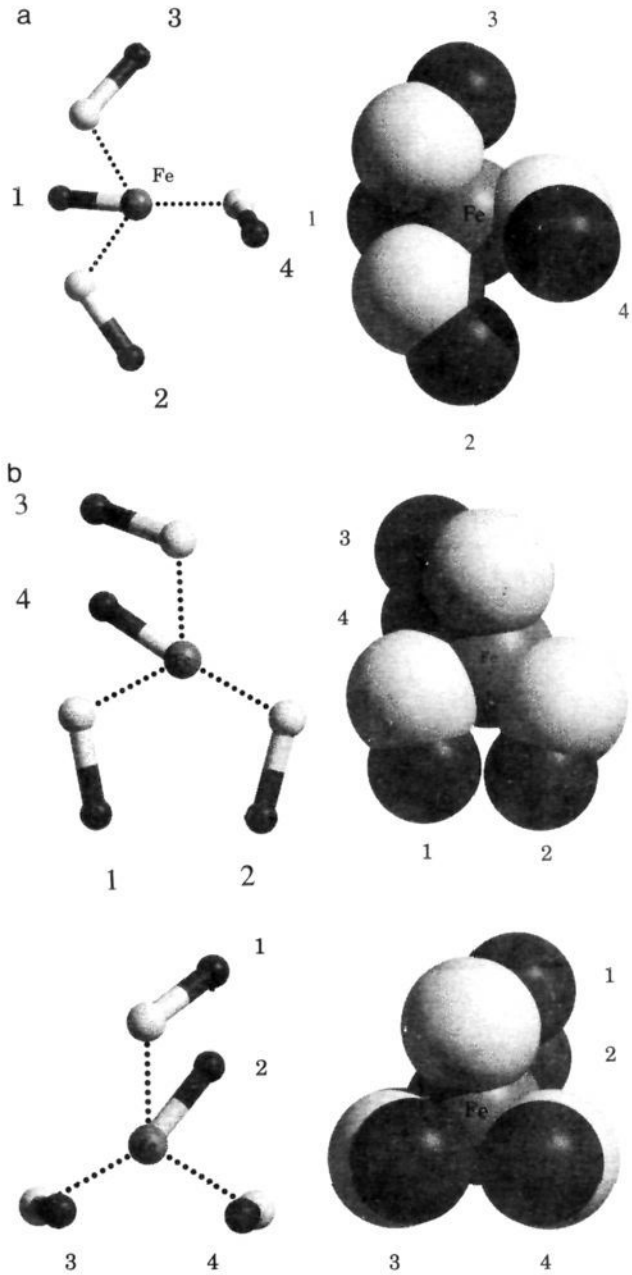

Figure 1. Configurations of the redox site with the dihedral angles of (a) the protein (upper representations) and (b) the Holm–Ibers analog open face (middle representations) and blocked face (lower representations), with only $Fe(SC)_4$ shown. In each, the figure on the left is a ball-and-stick representation and the figure on the right is a space-filling representation in the same orientation, where the carbon is shaded the darkest, the iron intermediate, and the sulfurs the lightest.

(9) Shenoy, V. S.; Ichiye, T. *Proteins: Struct., Funct., Genet.*, in press.
(10) Jorgensen, W. L. *J. Am. Chem. Soc.* **1981**, *103*, 335, 341, 345.
(11) (a) Bader, J.; Chandler, D. To be submitted for publication. (b) Schreiber, H.; Steinhauser, O. *Biochemistry* **1992**, *31*, 5856. (c) Smith, P. E.; Pettitt, B. M. *J. Chem. Phys.* **1991**, *95*, 8430.

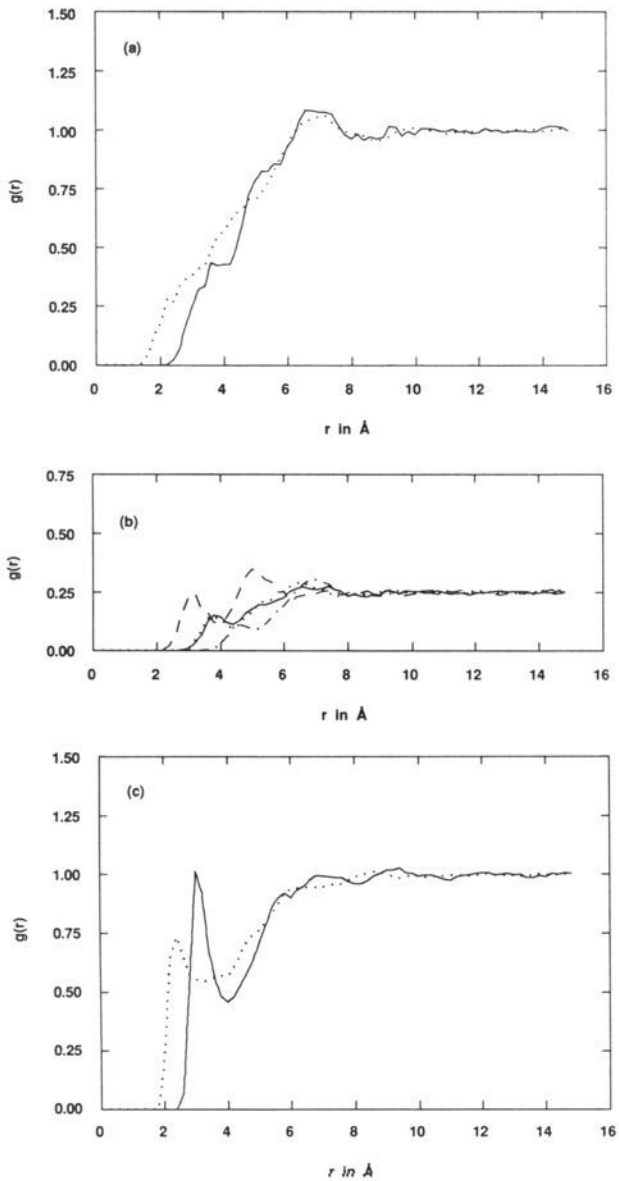

Figure 2. Radial distribution functions of water around the analog. (a) Water O and H around the Fe, *i.e.*, g_{FeO} (solid) and g_{FeH} (dot), respectively. (b) Water O around the Fe, *i.e.*, g_{FeO}, in which the function is calculated separately for each face formed by the sulfurs of the FeS_4 tetrahedron. For each face, only waters which are closest to that face are included; S^2:S^3:S^4 (dash), S^1:S^3:S^4 (dot), S^1:S^2:S^4 (dot–dash), and S^1:S^2:S^3 (solid) (see text for nomenclature). (c) Water O and H around the sulfurs, *i.e.*, g_{SO} (solid) and g_{SH} (dot), respectively, averaged over all four sulfurs.

actual run, the rest remain *trans*, and the fluctuations for all four angles are between 9.5 and 11°. Because of the dihedral transition in the equilibration, there are two rubredoxin-like ("Rd-like") faces, S^1:S^3:S^4 and S^1:S^2:S^3, which are partially blocked by one CH_2 and two $[Fe(S_2\text{-}o\text{-}xyl)_2]^-$-like ("HI-like") faces, S^2:S^3:S^4 and S^1:S^2:S^4, which are blocked by zero and two CH_2 groups, respectively.

(b) Structure of the Water Surrounding the Analog. The radial distribution functions of O and H around the Fe, *i.e.*, g_{FeO} and g_{FeH}, respectively, are given in Figure 2a. To provide a reference of the extent of the molecule, we note that the average distance between the Fe and the CH_3 groups during the simulation is about 4 Å, and the van der Waals diameters of the CH_3 and water are about 2.1 and 1.4 Å, respectively. We can then define the maximum extent of the analog as about 6 Å, so that the closest a water can be while remaining outside this distance is about 7.5 Å. Thus, the water may be divided into two main areas: the inner hydration shells which are within the average extent of the analog and the full hydration shells outside the analog. The water in the inner hydration shells is relatively structured. By integrating the area of the first peak in g_{FeO} (between 2 and 4 Å), it appears that about 2.3 water molecules are in the innermost shell. The most probable position of the O is at about 3.6 Å. The second peak in g_{FeO} (between 4 and 6 Å) indicates another 18 water molecules in the second inner shell. A third peak in both g_{FeO} and g_{FeH} can be seen between 6 and 8 Å. The water which is completely outside the analog appears almost structureless.

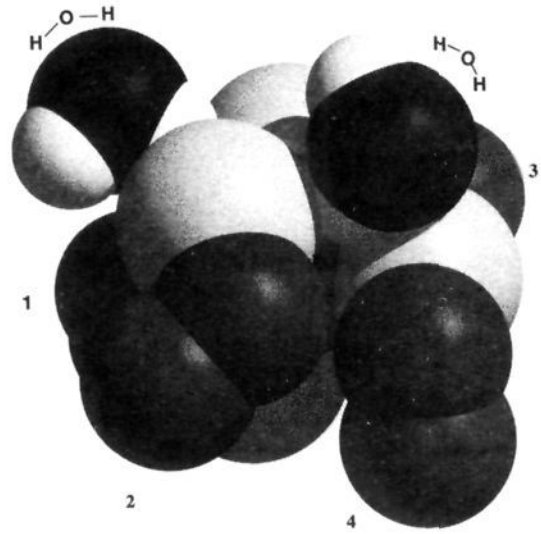

Figure 3. Configuration showing $Fe(SCH_2CH_3)_4^-$ and two water molecules within 4 Å of the Fe at 65.95 ps, where the water molecule on the left is 3.90 Å from the Fe and $\theta = 44°$ and the water molecule on the right is 3.19 Å from the Fe and $\theta = 48°$. The shading is as for the space-filling model in Figure 1 for the analog, and the waters are labeled.

Since the relative accessibility of each face of the FeS_4 tetrahedron to water is determined by the C^m–S^m–Fe–S^n dihedral angles, it is of interest to determine how many waters are present at each face and how close they come. In Figure 2b, the g_{FeO} is calculated separately for each face, in which only the waters which are closest to that face are included. Thus, the sum of the four g_{FeO} for each face will give the g_{FeO} in Figure 2a. From this figure, the two partially blocked Rd-like faces, S^1:S^3:S^4 and S^1:S^2:S^3, each have about 0.6 water (integrating between 0 and 4.0 Å) within the first shell (or about 1 each integrating to the first minimum at 4.4 Å), with a maximum value at about 3.8 Å. The HI-like face which is completely free, S^2:S^3:S^4, has about 1.1 waters (integrating between 0 and 4.0 Å) which come in very close to the Fe, with a maximum value near 3.1 Å, and a second close water (integrating out to 4.5 Å). However, the HI-like face which is blocked by two CH_2 groups, S^1:S^2:S^4, has essentially no waters in the first shell.

One feature to note in the first shell is that the water is able to penetrate so that the oxygen is within about 2.2 Å of the Fe and the hydrogen within about 1.4 Å of the Fe, *i.e.*, contact distance. This is possible because of the relatively open structure of the tetrahedral complex and the opening of the face S^2:S^3:S^4 by the rotation of the dihedral C^1–S^1–Fe–S^4 (during equilibration) so that it becomes HI-like, since this penetration is seen only at that face. A better picture of the degree of penetration of the water into the analog can be seen from actual configurations taken from the simulation. An example of a configuration with two water molecules within 4 Å of the Fe is shown in Figure 3.

Another feature to note in the first shell is that there appears to be a linear hydrogen bond between the water and the Fe since the first peak in g_{FeH} is about 1 Å closer than the first peak in

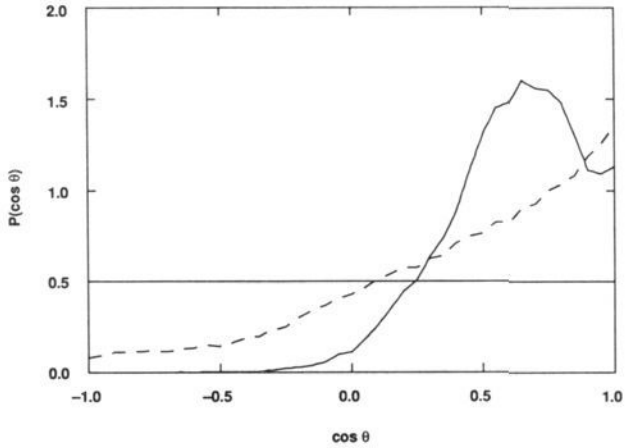

Figure 4. Probability of cos θ, $P(\cos\theta)$, versus cos θ for waters with oxygens within 4 Å of the Fe (solid) and the sulfurs (dash).

g_{FeO} and has about two hydrogens by integrating the area of the first peak in g_{FeH} between 1 and 3 Å. This can also be seen in Figure 3. This may seem unphysical considering that the Fe is formally Fe(III); however, the partial charge on the Fe is –0.05, since the electronic structure calculations indicate that the net negative charge of the Fe–S_4 site is delocalized over the entire site.[7a] To better describe the extent of reorientational polarization of a water molecule, we define θ as the angle between a line drawn from the Fe to the O and the perpendicular bisector of the H–O–H angle such that 0° corresponds to a bifurcated hydrogen bond. In Figure 4, we plot $P(\cos\theta)$, the probability of cos θ, versus cos θ for the innermost shell (within 2–4 Å of the Fe) around the Fe. It is apparent that the innermost shell is highly polarized. The maximum value of $P(\cos\theta)$ occurs at a value corresponding to one hydrogen pointing directly toward the Fe, much as is seen for simple singly charged ions.[12]

The radial distribution functions of O and H around the sulfurs (averaged over the four sulfurs), *i.e.*, g_{SO} and g_{SH}, respectively, are given in Figure 2c. By integrating the area of the first peak in g_{SO}, it appears that about 4.4 water molecules are within 4 Å of the sulfur. By looking at the radial distribution functions of the individual sulfurs, this is true for each individual sulfur except for S^1, which has only about 3.5 waters. The waters around a given sulfur are not necessarily exclusive of those around another, and included in these numbers are the two waters close to the Fe. The most probable position is at about 3.0 Å. However, the first peak of g_{SH} is less than 1 Å closer, and integrating it out to 3.2 Å shows about 5 hydrogens (4 for S^1). By examining $P(\cos\theta)$ around the sulfurs in Figure 4, it can be seen that the most probable configuration is a bifurcated hydrogen bond to the sulfur, although the preference over linear is not dramatic.

The effect of the immediate environment of the FeS site on the electrostatic potential at the Fe was also examined. While the composition of the total environment needs to be considered to obtain the full potential, the number, location, and polarity of the polar groups in the innermost shell can have a significant effect. Calculations indicate that while the rest of the environment has a large contribution to the absolute electrostatic potential, the *relative* electrostatic potentials of two different analogs are largely determined by the contribution of the innermost shells. The average electrostatic potential can be calculated by integrating the radial distribution multiplied by the potential. To examine the contribution of the innermost shell, the integration for the water O is carried out to 4.25 Å, and the integration for the water H is carried out so that the proper ratio of one O to two H is maintained. The contributions to the potential for the two HI-like faces are 17 kcal mol^{-1} e^{-1} for the S^2:S^3:S^4 face (1.37 waters)

(12) Dang, L. X. *J. Chem. Phys.* **1992**, *96*, 6970.

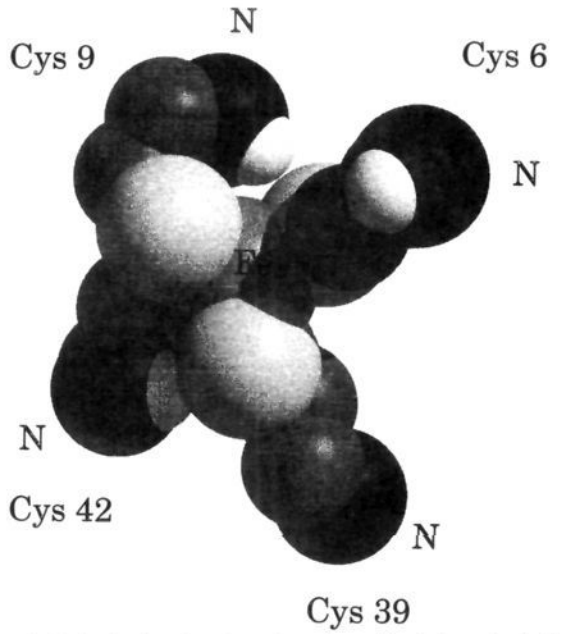

Figure 5. Rubredoxin redox site and nearby amides (where the shading is as for Figures 1 and 3 with the amides labeled). The two amides on the left side are the closest ones.

and 2 kcal mol^{-1} e^{-1} for the S^1:S^2:S^4 face (0.14 water), and for the two Rd-like faces 9 kcal mol^{-1} e^{-1} for the S^1:S^3:S^4 face (0.77 water) and 8 kcal mol^{-1} e^{-1} for the S^1:S^2:S^3 face (0.77 water), thus giving a total value of about 36 kcal mol^{-1} e^{-1}.

(c) Comparison with the Fe–S Site in Rubredoxin. In the crystal structure of *C. pasteurianum* rubredoxin,[2] no waters are seen in close contact with the Fe and the Fe is inaccessible via Lee and Richards surface accessibility criteria.[13] The closest water is 7.2 Å from the Fe (Fe–O distance). However, the arrangement of the protein polar groups (see Figure 5) bears some similarity to that of the water around the analog. For instance, the two amide nitrogens from Cys 9 and Cys 42 are both about 3.8 Å from the Fe, which is the same as the most probable distance of the water oxygens in the innermost shell of the analog for the Rd-like faces. The amide group from Cys 9 occupies the face formed by the S^γ from Cys 6, Cys 9, and Cys 42, and the amide group from Cys 42 occupies the face formed by the S^γ from Cys 9, Cys 39, and Cys 42. One difference is that although the protein dihedral angles would allow two more amides at this distance, the next closest amide nitrogens (or carbonyl oxygens) are more than 4.8 Å from the Fe. Another difference with the aqueous analog is that the geometries of Cys 9 and Cys 42 are more consistent with hydrogen bonds between the amide hydrogens and the S^γ of Cys 6 and Cys 39, respectively (Figure 5). The cosine of the angle between the amide bond and a line drawn between the N and the S^γ is almost 1 for both, whereas it about 0.7 for the analogous angle for the N and the Fe. Also, the N's are closer to the S^γ than to the Fe (the S^γ–N distance is about 3.5–3.6 Å vs the Fe–N distance of 3.8 Å), and the amide hydrogens are also closer to the S^γ (the S^γ–H distance is about 2.7 Å vs the Fe–H distance of 3.2 Å). Thus, all of the interatomic distances and angles are consistent with a linear hydrogen bond between Cys 9 NH and Cys 6 S^γ and between Cys 42 NH and Cys 39 S^γ.

The average electrostatic potential for the innermost shell can be calculated for the protein as was done for the analog. Here, the integration is carried out to 4.25 Å for the negative charges of the dipolar groups (*i.e.*, the amide N). For the remaining positive charges (*i.e.*, the amide H and C^α), the integration is carried out so that the proper ratio of positive to negative charge is maintained. Radial distribution functions from a simulation

(13) Lee, B.; Richards, F. M. *J. Mol. Biol.* **1971**, *55*, 379.

of rubredoxin[14] indicate that the contribution to the potential is about 11 kcal mol^{-1} e^{-1}, resulting from two amide groups.

Discussion

One important result obtained here is that, for tetrahedrally coordinated metal centers, the arrangement of the dihedral angles of attachment to the protein, such as the C–S–Fe–S angles in this study, determines how close the solvent can approach the Fe. By examining the simulation results for the radial distribution functions of the waters with respect to each of the faces, it appears that a face of the FeS_4 which is not blocked by any CH_2 groups will allow a single water to come to an average position of about 3.1 Å from the Fe, one which is blocked by a single CH_2 will allow a single water to an average position of about 3.8 Å, and one which is blocked by two CH_2 groups will essentially not allow water within the first 4 Å of the Fe. However, in the case of rubredoxin, the experimentally synthesized analog $[Fe(S_2\text{-}o\text{-}xyl)_2]^-$ is constrained to have different values for the C–S–Fe–S dihedral angles than the protein. Also, if the analog has dihedrals like those in $[Fe(S_2\text{-}o\text{-}xyl)_2]^-$, the water apparently can approach almost as close as the water in a solvated ferric ion, which is 6-fold coordinated by water at Fe–O bond lengths of 2.0 Å, which could affect the electronic structure of the FeS_4 complex.

A better comparison of the effects of environment on the redox potential of rubredoxin would be with an analog with the same C–S–Fe–S angles as the protein, but so far none have been made synthetically which are soluble in water without detergent. However, since the analog studied here has two faces like the protein and two like the synthetic analog, we can extrapolate these results to analogs with different C–S–Fe–S angles, by assuming that the total $g(r)$ (and thus the electrostatic potential) for an analog with a particular set of C–S–Fe–S dihedral angles may be estimated by summing the partial $g(r)$'s for each type of face from part b of the preceding section. This procedure is only an estimate as it ignores the effects on the $g(r)$ of any correlation between the faces, and further simulations are being carried out to verify these results. For instance, if these results are extrapolated to an analog with C–S–Fe–S dihedrals like those in rubredoxin with all four faces blocked by a single CH_2, they indicate about four waters at an average position of about 3.8 Å but none closer in than about 3 Å. Integrating out to 4.25 Å, the innermost shell would contribute 34 kcal mol^{-1} e^{-1} to the potential. Extrapolating again but now to an analog with C–S–Fe–S dihedrals like those in $[Fe(S_2\text{-}o\text{-}xyl)_2]^-$, the results indicate only about two waters at an average position of 3.1 Å from the Fe. Integrating out to 4.25 Å, the innermost shell would contribute 38 kcal mol^{-1} e^{-1} to the potential. Thus, these results indicate that a change in the C–S–Fe–S dihedrals of an analog from those of rubredoxin in those of $[Fe(S_2\text{-}o\text{-}xyl)_2]^-$ would give a substantial increase of 4 kcal mol^{-1} e^{-1} in the contribution of the innermost shell to the electrostatic potential. This is because the close approach of the first water to one of the HI-like faces at an average distance of 3.1 Å compared to the Rd-like faces at an average distance of 3.8 Å more than counterbalances the absence of an innermost shell water at the other HI-like face. Furthermore, while the contribution of the rest of the environment may not be well represented because of the short cutoffs used here, the contribution of outer layers will be become more similar with increasing distance from the Fe because the solute is essentially the same in both cases, and the contribution will also decrease in magnitude at the rate of the dipole interaction, so that the difference in the total electrostatic potential (*i.e.*, including all layers within a periodic box) may be estimated here from the simulation by integrating each $g(r)$ to half the box length. The difference in the total electrostatic potential is about 4 kcal mol^{-1} e^{-1} which agrees with the value calculated from just the inner shell.

So far, it has been impossible to compare how the protein affects the redox potential of the FeS_4 site relative to that of a bare site in water experimentally, since the only analogs synthesized up to now are not soluble in water and redox potentials have been measured only in DMF[3] and micelle aqueous solutions.[4] The simulation here provides the opportunity to do such a comparison. The results for the analog studied here can be examined in terms of the role of the protein matrix in determining its redox properties. Of course, the protein gives rise to an electric field at the redox site which is determined by the specific amino acid sequence and also controls the immediate environment of the redox site by simply excluding water from the Fe–S site by slightly burying it. Moreover, there is an obvious similarity between the immediate environment of the Fe–S site in the simulation of the analog in aqueous solution and in rubredoxin in that it consists of polarized groups in a polarized arrangement around the net negative charge of the Fe–S_4 site. Since the arrangement of NH···S bonds, which comprises the immediate environment of the Fe–S site, is thought to be important in controlling the redox potential of rubredoxin and other Fe–S proteins,[15] a detailed comparison of the inner shell of the Fe–S site in the analog vs the protein is made here. Of course, the total environment will influence the electrostatic potential, but because of the complex environment in the protein the discussion will be limited here to just the inner shell; a full description is given elsewhere.[14]

There are several factors which indicate that the protein matrix shifts the redox reaction more toward the oxidized state than for a bare FeS_4 site in water. The contributions of each factor individually in changing the inner shell contribution to the electrostatic potential from 11 kcal mol^{-1} e^{-1} in rubredoxin to an estimated 38 kcal mol^{-1} e^{-1} in an aqueous analog in the $[Fe(S_2\text{-}o\text{-}xyl)_2]^-$ conformation are given below. (Of course, the factors are coupled so that the contributions are not additive.) First, a major difference between the aqueous analog and rubredoxin is the replacement of the TIP3P waters (2.35 D) with the less polar amides (0.94 D), thus favoring reduction from the −1 to −2 state in the analog. Using the inner shell contributions to the electrostatic potential given in Results, changing the two nearby amides of the protein to water molecules at about the same distance (without allowing relaxation of the protein) can be estimated to increase the electrostatic potential by about 6 kcal mol^{-1} e^{-1}. Second, the protein prevents a close approach of dipole groups to the Fe because it constrains the dihedral angles C–S–Fe–S to values such that each face of the FeS_4 is partially blocked by a CH_2, thus favoring the oxidized state in the protein. Changing from the dihedral angles of the protein to that of $[Fe(S_2\text{-}o\text{-}xyl)_2]^-$ was estimated above to cause an increase of 4 kcal mol^{-1} e^{-1} in an aqueous analog, although a somewhat smaller increase would be expected in rubredoxin if it were possible to bring the amides closer due to the decrease in the polarity relative to water. Finally, the protein prevents more polar groups from coming in because the fold of the protein is such that only two of the four possible sites for polar groups (since the C–S–Fe–S angles of the protein will allow four close polar groups) are occupied, thus also favoring the oxidized state in the protein. If it were possible to put amides in all four sites, it would result in an increase in the potential of 11 kcal mol^{-1} e^{-1}.

An additional set of factors will also favor the oxidized state in the protein in that the location, number, and orientation of polar groups around the sulfurs are also important since the charges on all of the atoms of the Fe–S_4 site become more negative on reduction. One factor is that the waters in the analog are much closer to the sulfurs (r_{SO} = 3.0 Å) than the amides in

(14) Yelle, R. B.; Beck, B. W.; Ichiye, T. Unpublished results.

(15) Adman, E.; Watenpaugh, K. D.; Jensen, L. H. *Proc. Natl. Acad. Sci. U.S.A.* **1975**, *72*, 4854.

rubredoxin (r_{SN} = 3.5–3.6 Å). Also, the number of close oxygens (4.4) to the sulfurs in the analog is greater than the number of close nitrogens (3) to the sulfurs in rubredoxin.

Although we have not studied the analog in DMF, we would predict that, for $[Fe(S_2\text{-}o\text{-}xyl)_2]^-$, at most two molecules of DMF could be in the inner shell of the redox site, at an average distance much larger than the closest amide groups in the protein crystal structure. This, coupled with the lower dipole moment of DMF with respect to the similar peptide group, would indicate that the protein would favor reduction over $[Fe(S_2\text{-}o\text{-}xyl)_2]^-$, which is consistent with experimental redox potentials. This is an improvement over arguments based on the Born approximation for the solvation energy using the dielectric of DMF and estimates of the dielectric of a protein (from 2 to 10), which incorrectly predict the opposite trend.

The orientation of the dipoles will also influence the electrostatic potential, with linear hydrogen bonds to the Fe and bifurcated hydrogen bonds to the sulfurs favored in the aqueous analog and linear hydrogen bonds to the sulfurs favored in rubredoxin. The presence of linear hydrogen bonds to the sulfurs rather than the Fe in the crystal structure of the protein might seem to indicate that the water hydrogens pointing to the Fe in the analog simulation are due to an incorrect partial charge distribution. However, a structure obtained by minimizing the crystal structure with CHARMM19 parameters supplemented by the same energy parameters for the Fe–S site as used in the analog simulation gives similar results for interatomic distances and angles as seen in the crystal structure. Another possible explanation is that hydrogens of polar groups that are somewhat farther out (for instance, between 3.5 and 4. Å from the Fe) point to the sulfurs but those farther in point to the Fe so that, on average, the waters between 2 and 4 Å would point to the Fe. However, analysis of the analog simulation shows that the waters between 3.5 and 4 Å from the Fe have hydrogens pointing to the Fe rather than the sulfurs as well. The explanation seems to be that a water which has a bifurcated bond to a sulfur can also be oriented so that it also has a linear hydrogen bond to the Fe and also that the protein restrains the orientation of the amides.

Conclusions

A molecular dynamics simulation of a rubredoxin redox site analog, $Fe(SCH_2CH_3)_4^-$, in aqueous solution has been performed. The structure of the water is polarized by the net negative charge of the analog, as expected. However, there are several notable features of the solvation. First, water is able to penetrate to within contact distance of the Fe due to the open tetrahedral structure of the Fe–S site. The oxygen and hydrogen can come as close as 2.2 and 1.4 Å, respectively, of the Fe, which is closer than the Fe–S bond length of 2.26 Å. This would not be possible in Fe compounds with higher coordination numbers because of steric hindrance of the ligands. Also, it occurs only when there are faces of the FeS_4 tetrahedron which are not blocked by CH_2 groups. Second, for the analog simulated here, the average position of the oxygen is about 3.6 Å from the Fe, but only 2.3 oxygens are in the first peak of g_{FeO}, even though there are four equivalent faces for close approach in a tetrahedral structure. The CH_2 groups which break the tetrahedral symmetry are responsible for blocking some of the faces, so that the C–S–Fe–S angle determines the accessibility of a face. Third, the innermost waters have linear hydrogen bonds pointing directly at the Fe, and of the 4.4 waters in the first shell around each sulfur, the hydrogens generally point toward the sulfurs with a slight preference for a bifurcated hydrogen bond. An explanation for the linear hydrogen bond by water to the Fe is that a water can have both a linear hydrogen bond to the Fe and a bifurcated bond to a sulfur. Fourth, there appears to be a substantial difference in the electrostatic potential at the Fe between an analog in the conformation of rubredoxin and one in the conformation of $[Fe(S_2\text{-}o\text{-}xyl)_2]^-$, the best synthetic analog for rubredoxin. Finally, rubredoxin appears to favor the oxidized state over several possible analogs in aqueous solution, not only because the protein polar groups are less polar than water, but because the C–S–Fe–S angles are such that very close approach is not favored and because, given these angles, not all of the possible inner shell sites are filled.

Acknowledgment. This work was supported by grants from the National Science Foundation (DMB9010266), the American Chemical Society—Petroleum Research Fund (23983-G6), and the National Institutes of Health (1 R29 GM45303-01A1) and funds from Washington State University. The molecular images were generated using the program Preras3d/Raster3d by D. Bacon, A. Berghuis, M. Israel, and M. Murphy.